



1 Integrated Geophysical Analysis of Rangpur Saddle: Insights on Tectonics and 2 Magnetic Mineral Potential of North-Western Bangladesh

3
4 Mohammad Tawhidur Rahman Tushar¹, Asif Ashraf², Md. Mahfuz Alam¹, Md Nasif Jamil¹, Saba Karim¹,
5 Md. Shahjahan³, Md. Anwar Hossain Bhuiyan¹

6
7 ¹Department of Geology, University of Dhaka, Dhaka-1000, Bangladesh

8 ²Department of Earth Sciences, University of Oregon, Eugene, Oregon-97401, United States of America

9 ³Geological survey of Bangladesh, 153 Pioneer Road, Dhaka-1000, Bangladesh

10
11 *Correspondence to: Mohammad Tawhidur Rahman Tushar (mtrt@du.ac.bd) and Asif Ashraf (aashraf@uoregon.edu)*

12 13 Abstract

14
15 The northwestern region of Bangladesh holds untapped potential for magnetic mineral deposits at
16 shallow depths. Unlike much of Bangladesh, characterized by thick sediments of Bengal Basin,
17 this area is an extension of the Indian Shield, often referred to as the Stable Platform. It is also
18 geologically distinct, hosting structures related to the breakup of Pangea. The geology and
19 tectonics of this region have remained largely understudied. To address this gap, this study
20 integrates gravity, magnetic, seismic, and drilling data to investigate the subsurface structure and
21 evaluate the resource potential of the area. We utilize advanced filtering and modeling techniques,
22 including tilt derivatives and horizontal gradient methods, to understand the tectonic framework
23 and geometry of the subsurface structures. Our spatial analysis, using multiple geophysical
24 datasets, reveals distinct magnetic anomalies characterized by alternating magnetic highs and lows,
25 which we attribute to gabbroic intrusions along extensional faults that define the region's horst and
26 graben structures. To validate our interpretations, we developed an integrated 2-D subsurface
27 model that aligns with the observed geophysical data. However, the study is limited by the
28 availability of high-resolution seismic data and the sparse distribution of drilling locations, which
29 may affect the precision of our subsurface characterization. Our findings provide crucial insights
30 into the tectonic evolution of the stable platform and underscore the economic potential of the
31 Rangpur Saddle, the shallowest part of the stable platform, for mineral exploration. These insights
32 pave the way for further exploration and development initiatives focused on uncovering the
33 mineral wealth of this underexplored region.

34 35 1. Introduction

36
37 The northwestern part of Bangladesh is rich in potential mineral resources. The geological
38 diversity of this area suggests the presence of other valuable minerals that remain largely
39 unexplored (Akhtar, 2005; Hasan et al., 2023; Moon, 2022). In this area, basement rocks are
40 discernible at relatively shallow depths of 128 meters, hosting a spectrum of economic mineral
41 resources, including coal, limestone, white clay, and hard rock (Khan & Rahman, 1992). Notably,
42 Pirganj in the Rangpur district (**Figure 1**) records the country's highest magnetic anomaly
43 suggesting the potential for magnetic mineral ore deposits. In the 1990s, drilling activities were
44 conducted in the region after developing a 2D subsurface model by the Geological Survey of
45 Bangladesh (GSB) in collaboration with the United States Geological Survey (USGS). Despite
46 these efforts, no noteworthy ore body was identified during the drilling process (Rahman & Ullah,



47 2009). Moreover, the tectonic evolution of the Paleo-Proterozoic basement in the northwest region
48 of the Bengal Basin still needs to be studied.

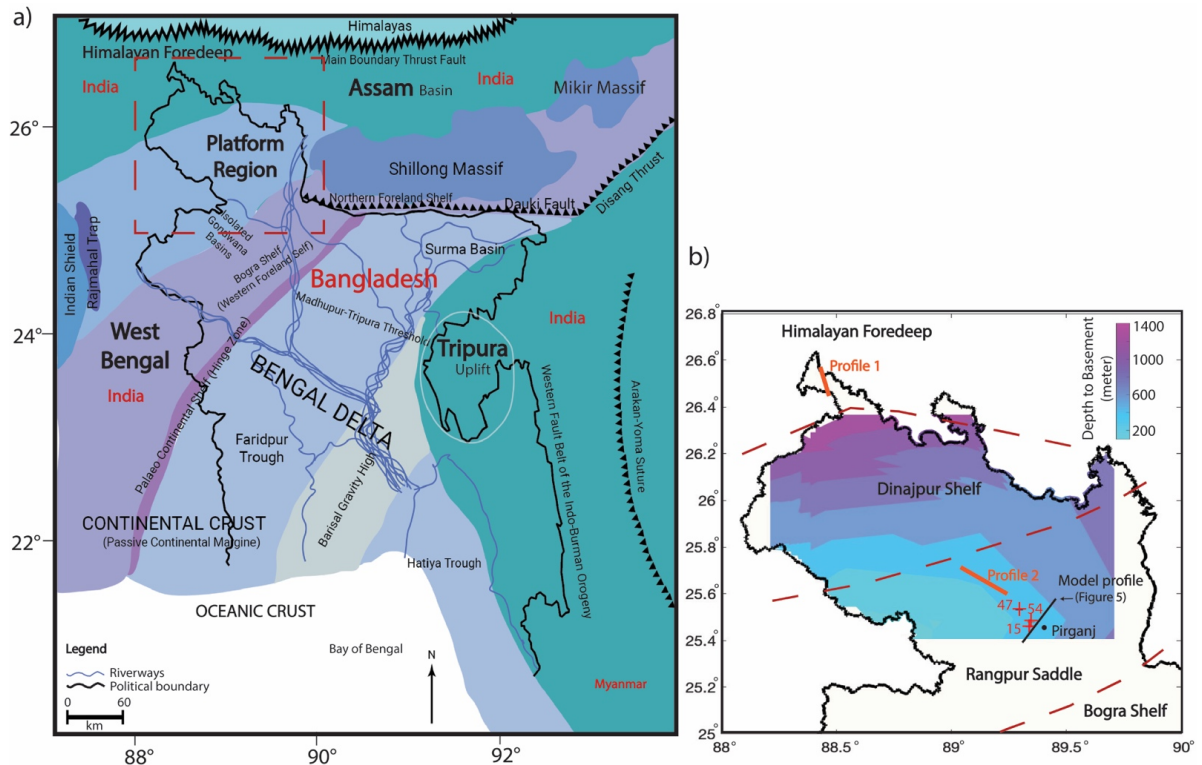
49

50 The study area is located in a region commonly referred to as the Rangpur platform or saddle
51 (Masum et al., 2021), an eastern extension of the Indian Shield (Alam et al., 2003). The northern
52 part of the Rangpur Saddle rests on a shallow Precambrian basement, ranging from 130 to 1000
53 meters in depth. This area of Bangladesh is geologically stable, characterized predominantly by
54 horsts and grabens, which were formed during the Cretaceous rifting of the Indian plate from the
55 Antarctica-Australia section of Gondwanaland (Curry, 1991; Curry & Moore, 1974). Although
56 the basement primarily consists of diorite, tonalite, and granodiorite, it is also intersected by
57 pegmatite and mafic/ultramafic dykes (Hossain et al., 2007; Kabir et al., 2001).

58

59 In this study, we explore the possibility of mafic dykes as the source of high magnetic anomalies
60 using multiple geophysical datasets while establishing the regional geological structure of this
61 significantly understudied area. We aim to conduct integrated spatial analysis and develop
62 subsurface models with gravity, magnetic, seismic, and drilling data to understand the regional
63 geological features. Gravity and magnetic data are widely used to understand and characterize
64 geological formations, particularly for identifying thin magnetic layers or faults (Adebiyi et al.,
65 2023; Jaffal et al., 2010). High-resolution potential field data help identify structures related to
66 local-scale mineralization that are covered by shallow alluvium or other unconsolidated sediments
67 (Hendrickson, 2016; McCafferty et al., 2014). Since potential field data can yield multiple
68 solutions (Filina et al., 2019). We also incorporate seismic and drilling data to constrain the
69 subsurface framework and produce more reliable results (Sundararajan, 2012). Our study applies
70 various filters to magnetic and gravity data to enhance and delineate regional crustal structures,
71 with a focus on highlighting structure edges where metallic mineral deposits are likely to be found
72 (Hildenbrand, 2000).

73



74
75 Figure 1: (a) Regional geological map of Bangladesh adopted from Hossain et al. (2019), illustrating various
76 geological and tectonic zones with distinct color coding. The names of neighboring countries are labeled in red. The
77 red dashed box indicates the study area in the northwestern part of Bangladesh. (b) The map of the northwestern
78 Bangladesh region shows basement depth with its tectonic subdivisions. Regional basement depths are collected from
79 GSB and constructed from various seismic reflection surveys. Red dashed lines mark the approximate boundaries of the
80 tectonic divisions. Seismic profiles (orange lines) and drilling locations (red plus signs) utilized in this study are
81 also highlighted. Our specific study area, Pirganj, is also shown on the map, where the highest magnetic anomaly is
82 observed. The integrated 2-D modeling profile of this study is also shown in this map with a solid black line.
83

84 2. Geological setting

85
86 Bangladesh, though geographically compact, possesses a complex and diverse geological
87 framework shaped largely by its position within the Bengal Basin (Roy and Chatterjee, 2015). This
88 region is primarily divided into two major tectonic units (Morgan and McINTIRE, 1959). To the
89 northwest of the hinge zone (see **Figure 1a** for location), the stable platform region features a
90 shallow basement composed predominantly of Precambrian-aged rocks (Uddin and Lundberg,
91 1998). Conversely, the southeastern portion of the Bengal Basin comprises a geosynclinal basin,
92 distinguished by significant sediment accumulation, with sediment thicknesses exceeding 12
93 kilometers (Alam, 1989). This tectonic configuration highlights the geological contrasts between
94 the stable platform and the more dynamic, subsiding basin to the southeast.
95

96 The Bengal Basin, encompassing Bangladesh and parts of the neighboring Indian states of West
97 Bengal, Assam, and Tripura, is situated at the northeastern edge of the Indian craton. It is one of



98 South Asia's largest peripheral collisional foreland basins, with a sedimentary sequence spanning
99 from the Early Cretaceous to the Holocene (DeCelles, 2011). The study area, located in the
100 northwest part of the basin and known as the stable platform, consists of three geological
101 components (Hossain et al., 2019): the Dinajpur Shelf, Rangpur Saddle, and the Bogra Shelf
102 (**Figure 1b**). The Himalayan Foredeep region, located just north of the Dinajpur Shelf, contains
103 the deepest basement in the stable platform (**Figure 1b**) and hosts numerous faults associated with
104 extensional tectonics (**Figure 2a**). South of the Foredeep region, the Dinajpur Shelf gently slopes
105 northward toward the Himalayan Foredeep at an angle of 1-3 degrees and is covered by recent
106 sedimentary deposits. The Rangpur Saddle, the southern block of the Dinajpur Shelf, connects the
107 Indian Shield to the Shillong Plateau and contains the shallowest basement in the Bengal Basin
108 (Jain et al., 2020) (**Figure 1b**). The Bogra Shelf, on the southern slope of the Rangpur Saddle, is
109 formed during the Early Cretaceous rifting of the Indian plate from Gondwana (Alam, 1989; Alam
110 et al., 2003). Both the Rangpur Saddle and Bogra Shelf host several horsts and graben, and half-
111 graben basins (**Figure 2b**).

112
113 The entire north-eastern Bangladesh is geologically stable with minimal folding impact that can
114 be traced back from Rodinia and Luna or Colombia supercontinents (Ameen et al., 2007; Zhang
115 et al., 2012). Ameen et al. (2007) suggest that the basement is a separate micro-continental
116 fragment trapped during the northward migration of the Indian Plate, while Hossain et al. (2007)
117 propose that it is a continuation of the central Indian tectonic zone. During the Precambrian, only
118 the stable shelf of the Bengal basin was part of the Indian Plate within Gondwana. By the Middle
119 Jurassic (~170–175 Ma), the Indian Plate began drifting, and becoming isolated by the end of the
120 Paleocene (~55.9 Ma) (Hossain et al., 2019). During the Late Paleozoic–Mid Mesozoic, the stable
121 shelf was developed as an intra-cratonic rift basin with Gondwana sediments in graben structures,
122 followed by Kerguelen igneous activity and widespread Rajmahal Trap volcanism (Hossain et al.,
123 2019; Valdiya, 2016).

124
125 The basement in our study area is the shallowest part of the Stable Shelf, which is uplifted to a
126 depth of 128 m from the surface, overlain by the Plio-Pleistocene Dupi Tila Sandstone and
127 Madhupur Clay (Rahman 1987), and is mainly composed of crystalline rocks, including granite,
128 granodiorite, and gneiss (Alam et al., 2003; Hossain et al., 2007). There is no outcrop of
129 Precambrian basement in this area, and the commonly observed horst and graben structures control
130 the stratigraphic subdivision. The Precambrian basement in this region lies beneath thick Cenozoic
131 clastic deposits and is primarily felsic in composition, intersected by mafic-ultramafic and
132 occasional felsic dykes (Chowdhury et al., 2022). Fault-bound graben basins within the basement
133 contain Carboniferous rock units from the Permian Period (286 to 245 million years ago) called
134 Gondwana formation, marking the oldest sedimentary rocks in Bangladesh (Alam et al., 2003; Jain
135 et al., 2020). Above the Permian Gondwana formation is the Jurassic Rajmahal Trap Formation,
136 consisting of volcanic basalt strata (Alam, 1989; Roy and Chatterjee, 2015). The Shibganj
137 Trapwash Formation overlays it, formed through weathering and erosion of the underlying igneous
138 rocks (Khan, 1991).

139
140 The Rangpur Saddle serves as the subsurface extension of the Indian shield, stretching between
141 the Shillong Plateau to the east and the Rajmahal Hills to the west. Geophysical studies have
142 identified two major faults framing the Garo-Rajmahal gap: the Dhubri-Jamuna Fault (western
143 edge of Garo Hills) and the Rajmahal Fault (eastern edge of Rajmahal Hills) which encloses the



144 Rangpur saddle (Hossain et al., 2019). Tectonic activities, particularly extensional tectonics during
 145 continental rifting, have significantly disrupted the basement topography, forming numerous
 146 horsts and grabens (Ahamed et al., 2020; Khan & Rahman, 1992). Despite this, the study area
 147 remains predominantly flat with sediment covers (Khan, 1991) from the Pleistocene to Holocene
 148 period (Reimann and Hiller, 1993). Near the Rangpur Saddle, the eastern part of the Indian Shield
 149 includes three major tectonic domains: Singhbhum Craton, Singhbhum Mobile Belt, and
 150 Chhotanagpur Gneissic Complex (Mukhopadhyay and Matin, 2020). Singhbhum Craton is
 151 characterized by prolonged crustal evolution during the Archean, comprising lithologies such as
 152 granitoids and metamorphic rocks. Singhbhum Mobile Belt underwent accretion and modification
 153 through volcanics, dyke swarms, and various intrusive bodies in the Proterozoic. Chhotanagpur
 154 Gneissic Complex comprised mainly of gneisses, amphibolites, and granulites with mafic dyke
 155 swarms, forming a structurally complex mobile belt. The tectonics of this region can be
 156 characterized by intra-cratonic structural depressions between the uplifted tectonic blocks. Seismic
 157 reflection studies indicate that the Moho in this region is complex and laminated, suggesting a
 158 history of tectonic and magmatic activity (Valdiya, 2016). In the West Bengal basin, the Moho is
 159 relatively shallow and horizontal (at a depth of 36 km), while other nearby regions (e.g., Kutch
 160 basin) have a dipping Moho influenced by tectonic processes (Rangin and Sibuet, 2017).

161
 162 Magnetic minerals, particularly iron ore, are widely found across the Indian Shield. These iron
 163 deposits typically appear as metamorphosed banded iron or silica formations. In eastern India, the
 164 Precambrian iron ore of the Singhbhum-North Orissa region is a horseshoe-shaped synclinorium
 165 that contains the most significant iron deposits near Bangladesh. The first discovery of iron ore in
 166 Bangladesh is located on the Dinajpur slope of the Rangpur platform (Alam et al., 2003). Around
 167 30 km southwest of our study area, Masum et al. (2021) report iron ore-bearing basement rock
 168 about 30 km southwest of our study area, with the iron ores occurring as a thin, metamorphosed
 169 laminated layer.

170
 171 To understand the geological succession in Pirganj and its surroundings, we present a generalized
 172 lithological depiction using data from EDH-15 and GDH-54 drill holes (Table 1).

173
 174
 175

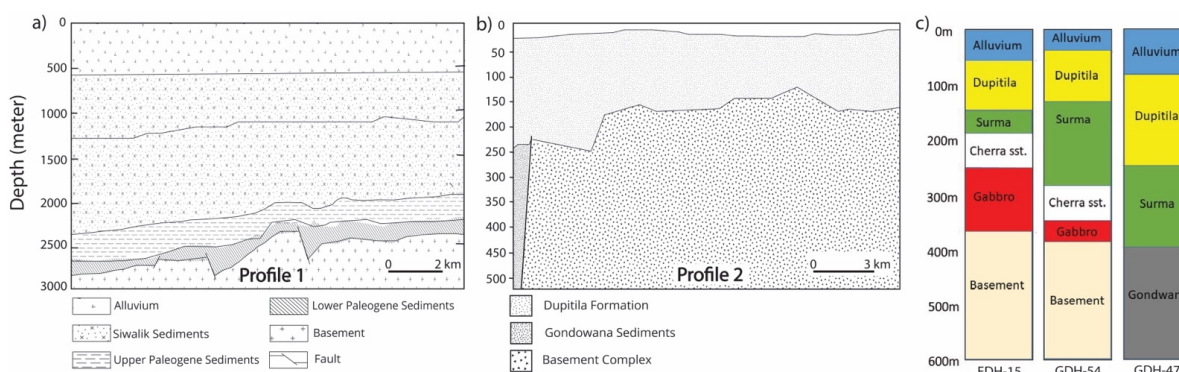
Table 1: Stratigraphic Succession of Pirganj & its adjoining Areas according to drill holes EDH-15 and GDH-54

Age	Rock Units	Lithology	Thickness (m)
Recent	Alluvium	Loose sand, medium to coarse-grained	52
Unconformity			
Pliocene	Dupitila	Sandstone(SST), silty SST, pebbly SST, pebbly bed; SST: medium to coarse-grained, pebbles: quartzite, gneiss & schist	33
Unconformity			
Late Oligocene to Early Miocene	Surma	Alteration of SST and shales and their combination, sand and silty shale. SST: fine to medium-grained; shale: soft and sticky	125
Unconformity			



Late Cretaceous to Paleocene	Cherra Sandstone	Sandstone: medium to coarse-grained	50
Unconformity			
	Basement	Gabbro; Diorite, quartz diorite, granodiorite, quartz monazite.	180+ (base not seen)

176
177



178
179
180
181
182
183
184

Figure 2: Seismic and drilling data used for integrated geophysical analysis in this study. (a) and (b) present interpretations of the two seismic profiles analyzed. (c) shows the drilling log data, which correlates with the 2D subsurface models and assists in spatial analysis. Refer to Figure 1b for their locations. Seismic profile 1 is from Himalayan Foredeep region while profile 2 represents Rangpur Saddle. All the drilling logs are situated near the highest observed magnetic anomaly in Pirganj, located in Northwestern Bangladesh.

185
186

3. Data and Methodology

187
188
189
190
191
192
193
194
195
196
197
198
199
200
201
202
203
204
205

In this study, we apply an integrative analytical approach utilizing multiple geophysical datasets for spatial analysis and 2-D subsurface modeling. Our primary datasets are potential field data, specifically gravity and magnetic data, provided by the Geological Survey of Bangladesh (GSB). We use Bouguer gravity data and total magnetic intensity data for our analysis. Topography data used in our geophysical modeling are obtained from the online repository of the Scripps Institution of Oceanography, which are derived from satellite altimetry (Smith and Sandwell, 1997). Additionally, we incorporate interpretations of seismic images obtained from GSB to correlate our findings from gravity and magnetic data. However, raw seismic images are unavailable, as private entities originally collected them. To further refine our 2-D integrated modeling, we use drilling data from three boreholes near our study area, also provided by GSB (see **Figure 1b** for the locations).

For geophysical spatial analysis, we use gravity and magnetic anomaly maps. The Bouguer gravity data from GSB are corrected for elevation. For the total magnetic intensity map, we apply a differential reduction to the pole (RTP) to adjust the magnetic grid (Arkani-Hamed, 2007). This correction involves computing magnetic inclination, declination, and total magnetic field values based on the International Geomagnetic Reference Field (Alken et al., 2021) with a magnetic epoch of 1980.



206 The next step in our spatial analysis methodology involves removing the regional trend from both
207 the gravity and magnetic data. This process, known as regional-residual separation, is essential for
208 isolating local anomalies by filtering out the broader, long-wavelength trends associated with
209 large-scale geological structures (Ashraf and Filina, 2023b; Kheyrollahi et al., 2021; Núñez-
210 Demarco et al., 2023). By removing these regional trends, we enhance the visibility of smaller-
211 scale or high-frequency anomalies, allowing subtle features and variations in the subsurface to be
212 highlighted more effectively. To remove regional anomalies, we apply an upward continuation of
213 1000 m to the Bouguer gravity data (**Figure 3a**). This approach simulates measuring the gravity
214 field at a higher elevation—1000 m in our case—effectively smoothing out high-frequency
215 anomalies associated with shallow or near-surface geological features (Balogun et al., 2023). For
216 RTP magnetic anomaly, we use a Gaussian filter to calculate the regional trend (**Figure 3b**). This
217 Gaussian filter acts as a low-pass filter, smoothing out high-frequency components in the dataset.
218 After extracting the regional anomaly from the potential field, we subtract it from the unfiltered
219 total anomaly, yielding the residual anomaly (**Figure 3**).

220

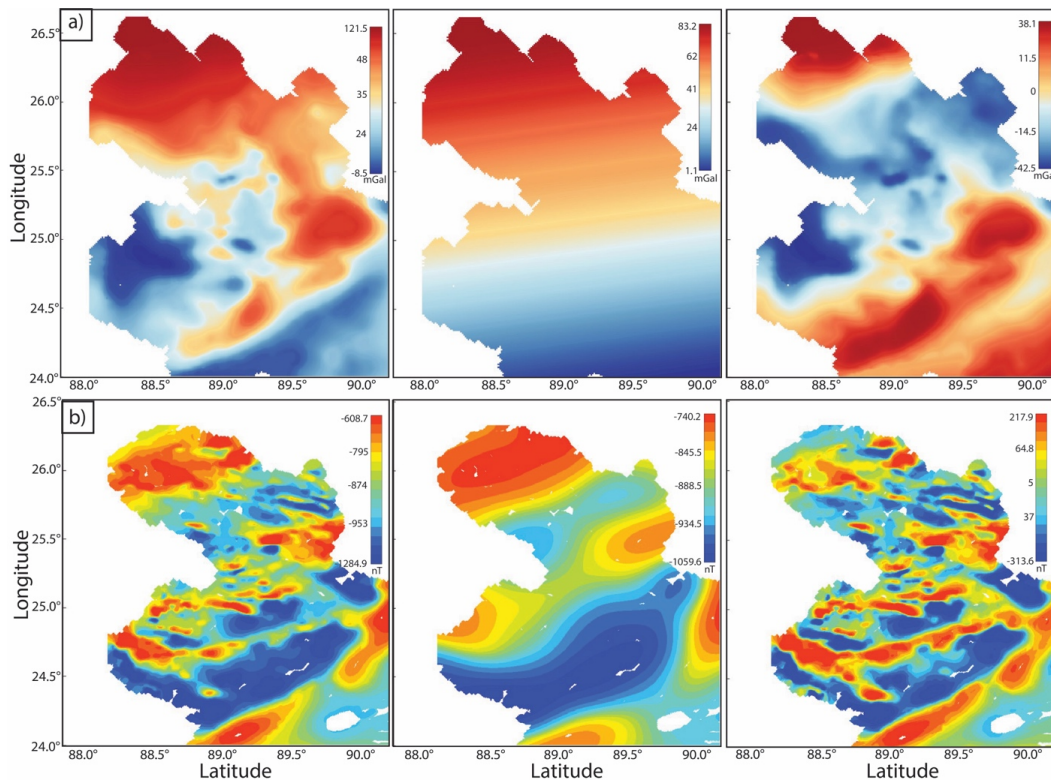
221 We apply several filters to the residual potential field data to enhance specific features and improve
222 interpretability (**Figure 3**). These filters involve various forms of derivative operations, which help
223 to highlight changes in the data that correspond to geological boundaries, faults, or other structural
224 details (Ibraheem et al., 2023; Ma et al., 2016; Nasuti et al., 2019; Núñez-Demarco et al., 2023).
225 For the residual RTP magnetic data, we apply and show two filters: the horizontal derivative and
226 the tilt derivative. The horizontal derivative filter, applied in x-direction (i.e., across the longitudes)
227 and y-direction (i.e., across the latitudes), accentuates lateral changes in the magnetic field, helping
228 to reveal abrupt variations. The tilt derivative filter, however, is especially effective as an edge
229 detector. It operates by combining both vertical and horizontal gradients, effectively highlighting
230 the edges of anomalous bodies. The tilt derivative produces values that tend toward zero over flat
231 regions, positive over rising areas, and negative over falling areas, creating a clear demarcation of
232 the edges of magnetic sources. As a result, this filter enhances the boundaries of anomalies and
233 helps pinpoint the locations and shapes of features with minimal distortion across varying depths
234 (Ashraf and Filina, 2023b; Pham and Oliveira, 2023). We apply the lineament mapping techniques
235 to map major structural boundaries from the filtered magnetic data (Ashraf & Filina, 2023a, 2023b;
236 Ogah & Abubakar, 2024; Zhang et al., 2024). Our approach focused on identifying gaps between
237 magnetic stripes, changes in the stripe orientation, and a significant reduction in stripe width. We
238 also calculate the analytical signals of the magnetic anomalies to highlight the areas with high
239 magnetizing amplitude (Nabighian, 1972; Roest and Pilkington, 1993) that may illuminate
240 magnetic mineral deposits (Mohamed et al., 2022). To calculate the analytical signal of the residual
241 magnetic data, we first compute the horizontal and vertical derivatives of the magnetic field in the
242 x, y, and z directions. The analytical signal was then derived by taking the square root of the sum
243 of the squares of these derivatives, yielding a map that represents the amplitude of the magnetic
244 field independent of direction and highlights the edges of magnetic sources. To validate our
245 interpretations, we cross-reference the magnetic lineaments with gravity data. Before validating
246 with gravity data, we filter the residual gravity data by applying the first vertical derivative and tilt
247 derivative to map major tectonic structures and delineate their boundaries.

248

249 We also develop 2-D integrated models of the subsurface to examine the variations in the physical
250 properties of the rocks (density and magnetic susceptibility). We build our models using the GM-
251 SYS module within the Geosoft software suite, employing a 2-D approximation (Geosoft, 2021).



252 The GM-SYS model is extended to +/- 30000 km (i.e., infinity) along the X-axis and 90 km along
253 the Z-axis to eliminate edge effects. By integrating gravity and magnetic data within this 2D
254 context, we can delineate major geological boundaries and assess regional structural trends with
255 sufficient accuracy for our research objectives. Our goal is to develop a simple subsurface structure
256 that satisfactorily aligns with gravity, magnetic, and logging data without introducing excessive
257 complexity that might overfit the potential field anomaly. Instead, we aim to replicate the general
258 pattern of the observed anomaly in our 2D modeling, seeking to generate computed anomalies
259 with comparable amplitude, wavelength, and phase to those observed in the potential fields.
260



261
262

263 Figure 3: Potential field data maps of northwestern Bangladesh used in this study to analyze geological and tectonic
264 features. (a) Gravity anomaly maps: from left to right, the Bouguer gravity anomaly, regional Bouguer gravity anomaly
265 with 1000 m upward continuation, and residual Bouguer gravity anomaly. (b) Magnetic anomaly maps: from left to right
266 the RTP total magnetic anomaly, regional magnetic anomaly after Gaussian filtering, and residual magnetic
267 anomaly.

268

269 4. Result

270

271 4.1 Integrated spatial analysis

272

273 In this study, we first establish the regional tectonic structures of northwestern Bangladesh through
274 spatial analysis of multiple geophysical datasets. We utilize gravity, magnetic, seismic image



275 interpretations, and drilling log data to characterize the tectonic setup of this region. Our analysis
276 of residual magnetic and gravity anomalies reveals that the Rangpur Saddle exhibits distinct
277 geophysical characteristics compared to its northern counterpart, the Himalayan Foredeep region.
278 These differences are discernible in the long-wavelength or broad-scale geophysical signatures
279 across the two regions.

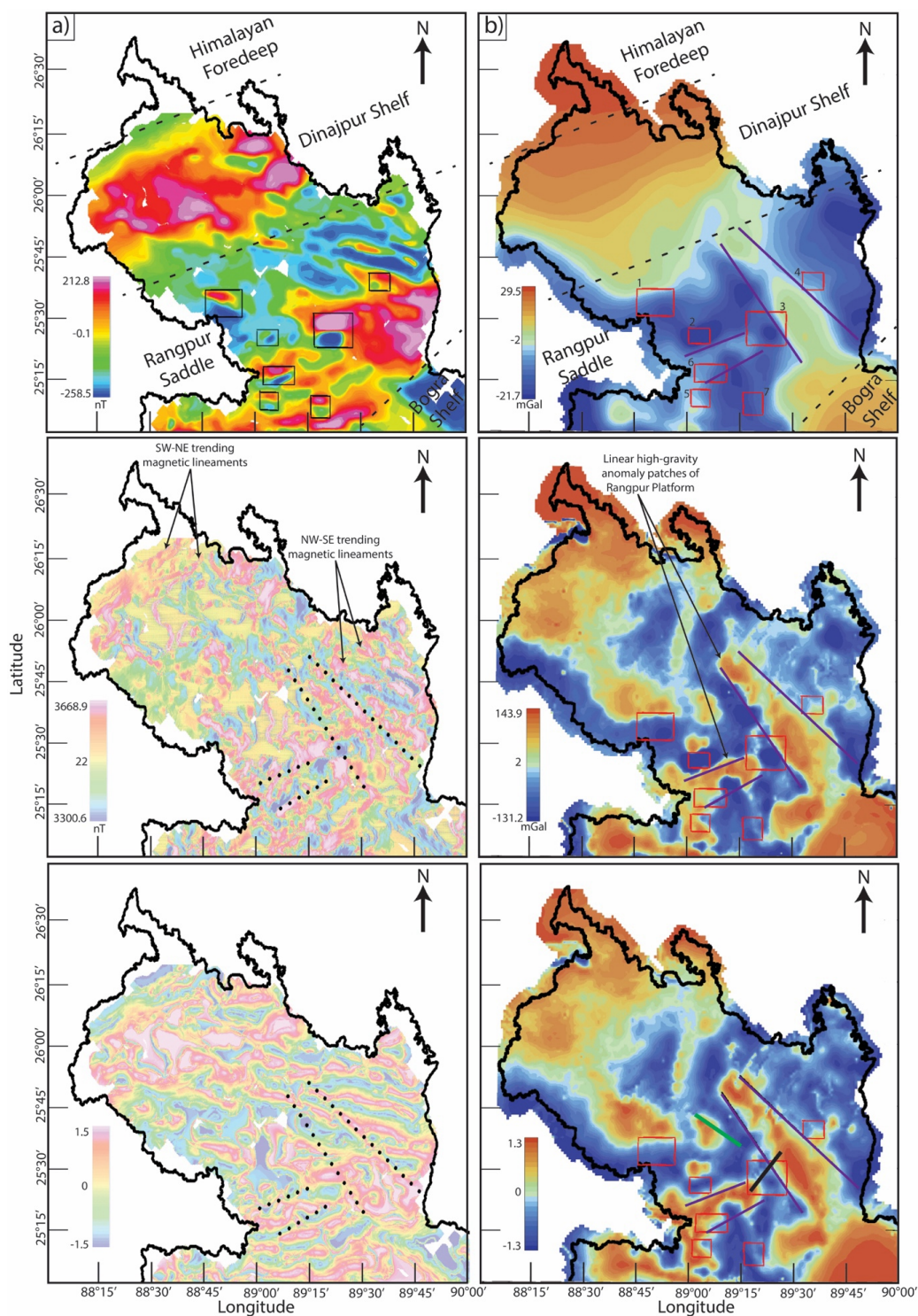
280

281 In the Himalayan Foredeep, north of 26°N latitude, we observe a high residual Bouguer gravity
282 anomaly, ranging from approximately 5 to 30 mGal. In contrast, the Rangpur Saddle, located south
283 of this latitude, is marked by a low residual Bouguer gravity anomaly, typically between -22 and
284 0 mGal. Similarly, the Rangpur Saddle shows lower residual RTP total magnetic anomalies,
285 ranging from 0 to 260 nT compared to mostly high magnetic anomalies in north (~ 0 to 215 nT).
286 The spatial patterns of these anomalies also differ across the regions. South of 26°N latitude, in
287 the Rangpur Saddle, the horizontal and tilt derivative magnetic anomalies show a predominance
288 of NW-SE trending magnetic lineaments. North of this latitude, in the Himalayan Foredeep, the
289 magnetic anomaly trend shifts predominantly to a SW-NE orientation. Additionally, in the vertical
290 and tilt derivatives of the gravity data, we observe the most pronounced high-gravity linear
291 anomaly patch trends NW-SE south of 26°N latitude, consistent with the magnetic anomaly trend
292 in this area. South of 26°30'N latitude, we see another linear high-gravity patch in the filtered
293 Bouguer gravity data trending NW-SE, indicating a different orientation than the other high-
294 gravity patch of the Rangpur Saddle region. These two high-gravity patches are also traceable in
295 the filtered magnetic anomalies, following the magnetic lineament mapping procedure.

296

297 Within the Rangpur Saddle region, we observe multiple semi-circular patterns characterized by
298 alternating magnetic highs and lows. From the RTP residual magnetic anomaly data, we identify
299 seven distinct patterns. The identification of these patterns follows several consistent criteria. First,
300 the alternating high and low anomalies are generally oriented in a north-south direction. Second,
301 each pattern features a magnetic high in the northern section and a corresponding low to the south.
302 Third, within each pattern, the size, area, and amplitude of the magnetic high and low anomalies
303 are comparable, contributing to a symmetrical structure. Mapping these magnetic patterns of
304 alternating highs and lows onto the filtered gravity maps reveals that they consistently lie near the
305 boundary between high and low gravity anomalies. While most of these magnetic patterns
306 (patterns 1, 4, 5, 6, and 7) intersect only one boundary, a few patterns (specifically patterns 2 and
307 3) touch boundaries on both sides.

308





310 Figure 4: a) Magnetic anomaly maps of northwestern Bangladesh. The top panel displays the residual RTP total
311 magnetic anomaly, the middle panel shows the first horizontal derivative in the x-direction (across longitudes), and
312 the bottom panel illustrates the tilt derivative. Black boxes highlight areas where semi-circular magnetic patterns of
313 alternating highs and lows are observed. Dotted black lines in the middle and bottom panels indicate boundaries of
314 high gravity regions. b) Bouguer gravity anomaly maps of northwestern Bangladesh. The top panel presents the
315 residual Bouguer gravity anomaly, the middle panel shows the first vertical derivative, and the bottom panel displays
316 the tilt derivative. High gravity regions are outlined by purple solid lines, and red boxes indicate areas with magnetic
317 patterns of alternating highs and lows. The solid green line in the bottom panel represents seismic profile 2 from Figure
318 2. The thick solid black line shows the 2-D integrated modelling profile of Figure 5.

319 4.2 Integrated subsurface modeling

320 We develop a 2-D subsurface model utilizing gravity, magnetic, and drilling log data (**Figure 5**).
321 The goal of this model is to approximate the observed anomalies on a local scale while aligning
322 with the available drilling log information (**Figure 2c**). Importantly, we do not aim to achieve a
323 precise fit between the observed data and calculated anomalies. This decision is driven by the fact
324 that the observed potential field data are influenced by regional structures, and without sufficient
325 seismic information, constructing a reliable regional model is not feasible. Instead, we focus on
326 developing a simplified version of the subsurface model that reasonably fits the observed
327 anomalies and drilling data.

328 To ground the 2-D model in reality, we incorporated available drilling log information (**Figure 2**).
329 Based on these logs, the model includes five sedimentary layers above a crystalline basement. The
330 shallowest layer is assigned as alluvium, extending to a depth of 50 meters or less. Beneath the
331 alluvium, we sequentially include the Dupitila, Surma, and Cherra sandstone layers. The variable
332 thickness of these sedimentary layers comes from the drilling log information, except for the
333 Gondwana layer. The thickness of Gondwana is approximated based on the gravity fit. Below
334 these layers, we model a mafic intrusion of gabbro, which occurs within fault structures that have
335 developed within the underlying felsic basement.

336 The resulting model indicates that a horst and graben structure is the most plausible configuration
337 when considering the regional geological context. This structural interpretation also provides a
338 reasonable match to the observed geophysical anomalies. Additionally, based on information from
339 drilling log GDH 47, we assign a layer of Gondwana sediments within the graben basin which is
340 contributing to the low observed gravity in this region.

341 Densities in the model are derived from drilling data, reflecting the unique lithological
342 characteristics of each unit. The alluvium, Dupitila, Surma, and Cherra Sandstone layers are
343 modeled with densities of 2000, 2200, 2500, and 2670 g/cm³, capturing their progressive
344 compaction and mineral composition. The Gondwana unit, enriched with coal deposits, exhibits a
345 notably lower density of 2200 g/cm³, consistent with its organic-rich composition. Beneath these
346 layers, the felsic basement and gabbroic intrusion stand out with densities of 2800 and 3000 g/cm³,
347 highlighting their denser crystalline structure and mafic origins.

348 Between 400 and 800 meters depth, the gabbroic intrusion begins to follow the fault plane. The
349 thickness of both the Gondwana layer and the underlying felsic basement is determined from the
350 amplitude of the calculated gravity and magnetic anomalies. The thickness of the Gondwana layer
351 influences the minimum value of the calculated gravity anomaly, while the amplitude of the
352

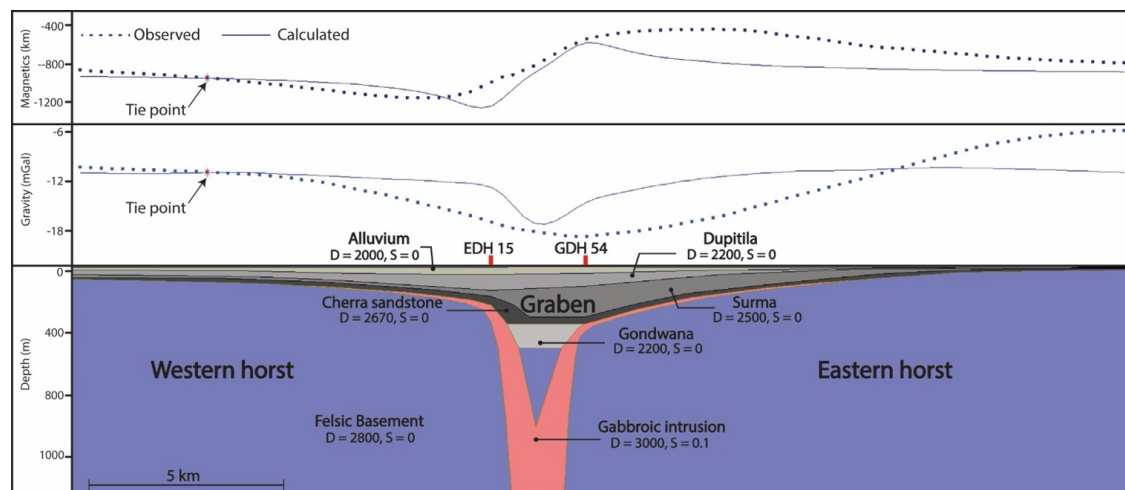


358 magnetic anomaly helps determine the depth of the gabbroic intrusion. Notably, our calculated
 359 anomalies are of high frequency. This occurs because our modeling does not incorporate all
 360 regional structures; instead, it focuses only on local structures. As a result, the calculated anomalies
 361 reflect primarily local or high-frequency potential field anomalies.

362

363 Our 2D subsurface model reveals two horst structures with a graben basin in the middle. We refer
 364 to these as the eastern and western horsts based on their geographic locations. In the model, the
 365 western horst structure is depicted as deeper, consistent with the observed gravity anomaly, which
 366 shows lower gravity in the western horst compared to the eastern horst. Our model does not include
 367 the larger horst structure on the eastern side, which likely explains the discrepancy between the
 368 calculated and observed anomalies over the eastern horst.

369



370

371

372 Figure 5: Integrated 2D geophysical model over the highest magnetic anomaly in northwestern Bangladesh. See Figure
 373 1b and 4c for the location of the model profile. The top panel presents the magnetic anomaly, and the middle panel
 374 shows the gravity anomaly, with observed (dotted) and calculated (solid) data. Tie points, marked by red stars, indicate
 375 where the calculated anomalies are vertically shifted to align with the observed data. The bottom panel illustrates the
 376 subsurface model, with geological units represented by distinct colors. 'D' denotes density (g/cm^3), and 'S' denotes
 377 magnetic susceptibility (SI units). The red vertical dashes show the location of the drilling logs used to constrain the
 378 subsurface units.

379

380 5. Discussion

381

382 5.1 Basement structure

383

384 One of the primary goals of this paper is to understand the basement structure and tectonic setup
 385 of the Rangpur Saddle. Our findings reveal significant differences in the basement structures of
 386 the Rangpur Saddle compared to its northern counterparts, evident in both gravity and magnetic
 387 data. A key distinction is the depth to basement between these regions (**Figure 1b**). Previous
 388 studies consistently suggest that the basement depth in the Rangpur Saddle is shallower than in the
 389 Dinajpur Shelf. However, those studies were based on limited seismic and drilling data. Our
 390 results, however, indicate a more complex basement geometry than previously understood.

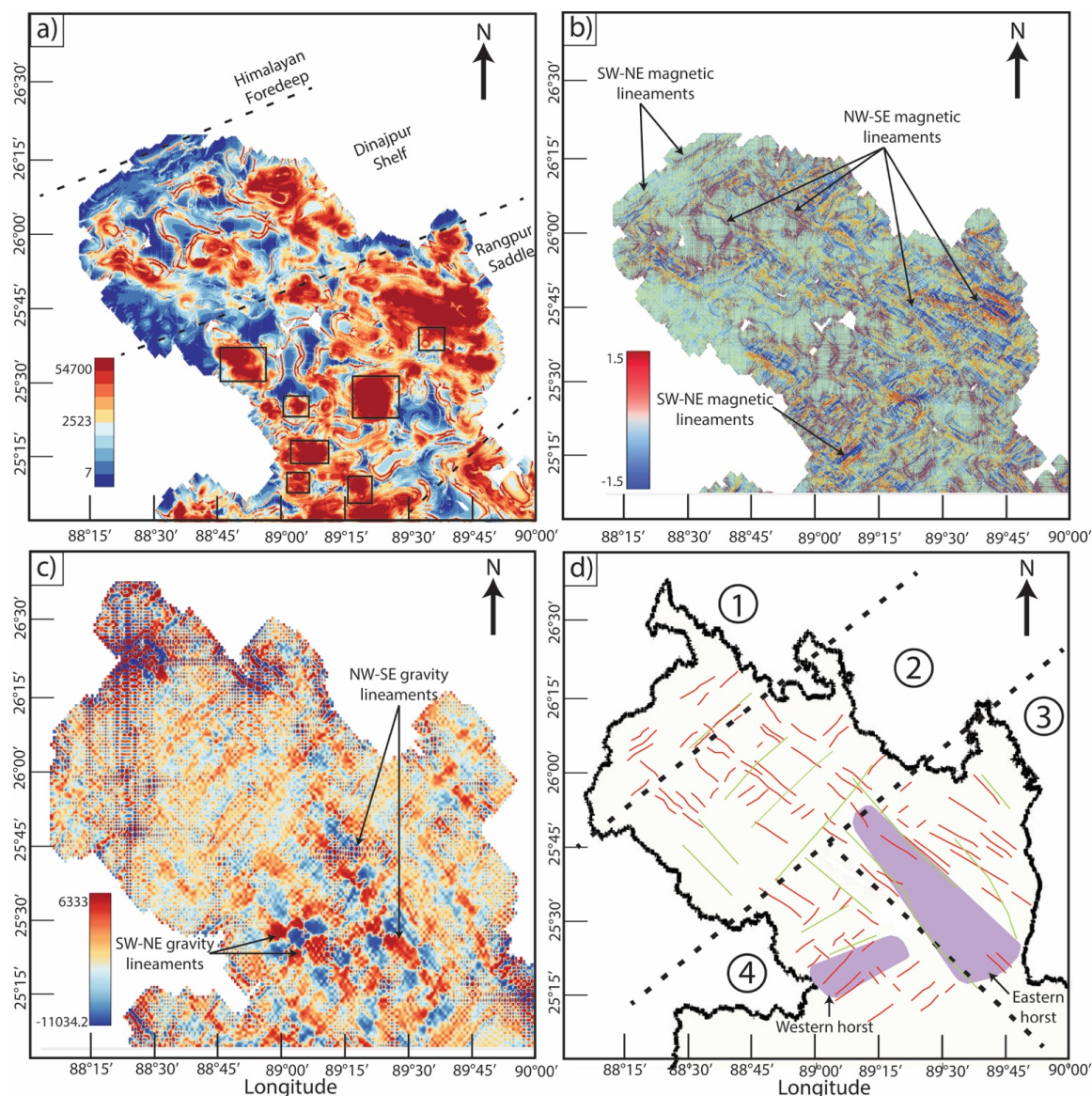


391 Filtered gravity and seismic data presented here suggest that the Rangpur Saddle region contains
392 both shallow and deep basement features (**Figure 4b**). Considering regional tectonics, we propose
393 that high gravity values correspond to shallow horst structures, while low gravity values indicate
394 deeper graben structures. However, the frequency of horsts and grabens is significantly lower in
395 the Rangpur Saddle compared to the northern Himalayan Foredeep and the Dinajpur Shelf (**Figure**
396 **2a & 2b**). In the Rangpur region, we identified only two horsts of notable width and length. The
397 boundaries of these horst structures also appear as lineaments in the filtered magnetic data (**Figure**
398 **4a**), suggesting the presence of major structural boundaries.

399
400 Furthermore, differences in the directions of magnetic lineaments between the Rangpur Saddle
401 region and its northern counterparts—the Dinajpur Shelf and the Himalayan Foredeep—suggest
402 variations in paleo-tectonic stress orientation (**Figure 4a, 6a & 6b**). Existing literature
403 characterizes northwestern Bangladesh predominantly with extensional tectonics (Royhan Gani
404 and Mustafa Alam, 2003). Near the Himalayan Foredeep boundary, SW-NE trending magnetic
405 lineaments indicate a paleo-principal stress direction oriented NW-SE. Moving southward into the
406 Dinajpur Shelf, NW-SE trending magnetic lineaments become more common (**Figure 6b**),
407 pointing to a shift in the principal stress direction associated with extensional tectonics. In the
408 Rangpur Saddle, these NW-SE trending lineaments are even more frequent, especially in the
409 eastern part, indicating a greater intensity of paleo-tectonic stress in this region compared to the
410 Dinajpur Shelf. Based on traced magnetic and gravity lineaments, the stable platform can be
411 divided into four distinct zones (**Figure 6d**). In Zone 1, located in the northern part, lineaments
412 predominantly trend SW-NE, with only a few exceptions. Moving southward into Zone 2, there is
413 a mixture of two differently trending lineaments: SW-NE and NW-SE. In Zone 3, in the
414 easternmost section of the stable platform, lineaments primarily trend NW-SE, aligning with the
415 eastern horst. Finally, in Zone 4, the southernmost region, lineaments generally follow an SW-NE
416 trend, corresponding with the western horst. This subdivision highlights the complex nature of past
417 tectonic processes in this region.

418
419 We also identify seven semi-circular patterns of alternating magnetic highs and lows. When
420 mapped onto gravity data, these patterns consistently align with the boundaries between high and
421 low gravity patches, indicating the boundaries between horsts and grabens. Drilling log data near
422 the most prominent magnetic anomaly reveals the presence of gabbro, which may explain these
423 alternating magnetic highs and lows. Furthermore, these regions of alternating magnetic patterns
424 also spatially correlate with overall high magnetization (**Figure 6a**). We propose that these gabbro
425 formations resulted from intrusions along normal faults, formed by extensional tectonics, which
426 define the boundaries between horsts and grabens.

427



428
429
430
431
432
433
434
435
436
437
438
439

Figure 6: Filtered potential field maps of the northwestern stable platform region of Bangladesh, highlighting major tectonic structures and boundaries. (a) Analytical signal map derived from the magnetic anomaly (methodology detailed in Sect. 3), showing magnetization amplitudes across the region. Black boxes indicate areas of semi-circular magnetic patterns with alternating highs and lows, as shown in Figure 4a. Dashed lines represent boundaries between established tectonic subdivisions. (b) Total horizontal gradient map of the magnetic anomaly, calculated by applying a first horizontal derivative filter in the X-direction, followed by a first horizontal derivative filter in the Y-direction. (c) Total horizontal derivative of the residual gravity anomaly. (d) Map displaying traced magnetic lineaments (in red) from 'b' and gravity lineaments (in green) from 'c'. Black dashed lines indicate regional subdivisions based on mapped tectonic lineaments. Purple polygons mark horst structures in the Rangpur Saddle, interpreted from filtered gravity data (refer to Figure 4b).



440 **5.2 Economic mineral potential**

441

442 Our integrated spatial analysis and 2-D modeling indicate that the Rangpur Saddle hosts at least
443 two significant horst and graben structures. The 2-D modeling results, corroborated by drilling log
444 data, confirm the presence of gabbroic bodies along the normal faults within these structures
445 (**Figure 7**). We propose that these gabbroic intrusions result from magmatic emplacement along
446 extensional faults, consistent with processes typically observed during the early stages of
447 continental breakup. The breakup process involved rifting events that progressively separated the
448 Indian subcontinent from the other Gondwanaland constituents (Veevers, 2004). Key rifting
449 episodes and magmatic activities, such as the formation of the Central Atlantic Magmatic Province
450 and related tectonic movements, facilitated this separation (Thompson et al., 2019; Veevers, 2004).
451 In such tectonic settings, normal faulting and rift-related subsidence create pathways for mafic
452 magmas to ascend (Brune et al., 2023; Pirajno and Santosh, 2014; Ruppel, 1995), leading to the
453 emplacement of gabbroic and other mafic intrusions within the crust (Magee et al., 2019).

454

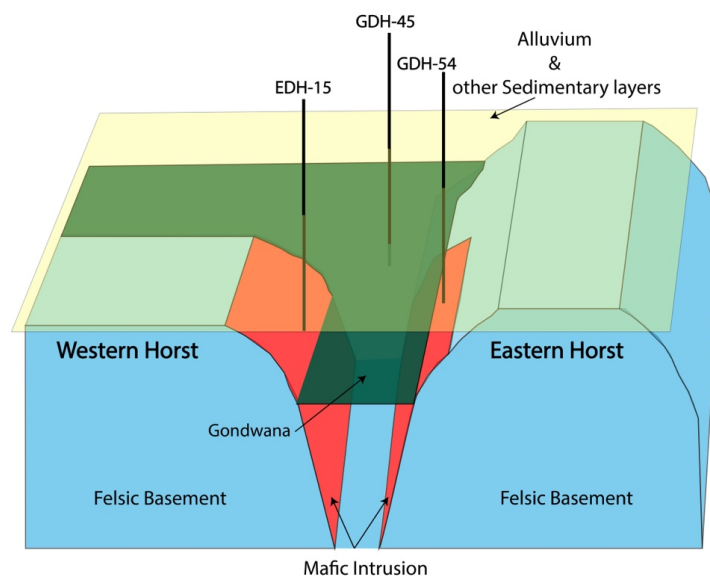
455 Mafic magma intrusions are commonly observed along extensional fault planes in tectonically
456 active regions worldwide. Troll et al. (2021) shows that in NW Scotland, Long Loch Fault acted
457 as dynamic magma conduit with its movements facilitating the ascent of ultrabasic magmas. These
458 magmas intruded along faults and fractures, leading to the destabilization and collapse of existing
459 cumulate layers, forming extensive breccias. A study on Mesozoic gabbroic intrusions in the High
460 Atlas Mountains highlights their emplacement along extensional faults during the rifting
461 associated with the Central Atlantic Magmatic Province, where more than 50% of gabbro samples
462 exhibit stable magnetization from magnetite which is identified as the primary component (Calvin
463 et al., 2017). Fuller & Waters (1929) have extensively studied horsts and graben structures in
464 southern Oregon where they found emplacement of volcanic and intrusive rocks are closely
465 associated with extensional faulting. These normal faults and the resulting grabens provide
466 pathways for magma to ascend and intrude, which is evident from the prevalence of rhyolitic,
467 dacitic, and andesitic vents as well as basaltic dikes aligned with the faults.

468

469 Mafic intrusions along fault zones are often associated with magnetic mineral deposits, which can
470 be economically significant as ore bodies (Zhou et al., 2005). For instance, magnetite deposits are
471 found within mafic intrusions along the fault planes in Egypt, which exhibit high magnetic
472 anomalies, facilitating their detection and delineation (Kharbish et al., 2022; Mousa et al., 2020).
473 Also, in Central Iran, iron-bearing magnetic mineral deposits are observed to exhibit high magnetic
474 and gravity anomalies (Kheyrollahi et al., 2021).

475

476 Based on current geochemistry data, the Rangpur Saddle holds significant potential for magnetic
477 mineral ore deposits, driven by its mafic-ultramafic sequences and iron-rich dykes (Ameen et al.,
478 2021). High Fe₂O₃ content in hornblendites and associated minerals like magnetite and ilmenite
479 indicate strong magnetization. The tectonic setting, with extensive magmatic intrusions, provides
480 ideal conditions for mineralization. These findings highlight the region as a promising target for
481 future exploration of magnetic ore bodies.



482

483

484

485

486

487

488

489

490

491

492

493

494

495

496

497

498

499

500

501

502

503

504

505

506

507

508

509

510

511

512

Figure 7: 3D schematic diagram illustrating the tectonic structures in Pirganj, where the highest magnetic anomaly is observed in Bangladesh. The felsic basement, depicted in blue blocks, includes two horsts, as shown in Figure 5d. Possible mafic intrusions along the faults are indicated in red. Sedimentary layers are represented by a single horizontal layer in specific colors, with the graben basin likely filled with Gondwana sediments shown in green, and other sedimentary layers, including alluvium, shown in yellow. The approximate locations of the three drilling logs used in this study (refer to Figure 1b for their locations) are also indicated.

5.3 Limitations and Future Research

Compared to other regions globally, limited published research exists for our study area, restricting our ability to draw on established models and findings. Situated at the eastern edge of the Indian Shield, this area transitions into a different tectonic subdivision, creating a tectonic complexity that cannot be fully resolved with the available low-resolution data. The scarcity of high-resolution datasets, such as regional-scale seismic surveys, further limits our capacity to delineate regional structures accurately. Additionally, the available well log data are predominantly shallow, reaching depths of approximately 500 meters, which limits insights into deeper geological and tectonic features beyond 2 kilometers. Petrographic descriptions of the basement rocks are also rudimentary, as they are primarily based on a limited number of well logs, most of which were drilled before the 1990s, leaving significant gaps in our understanding of the area's deeper subsurface geology.

Future research in this region will focus on developing 3D models of the subsurface, providing a more detailed understanding of its geological structure. This effort will include creating a comprehensive dataset repository that incorporates historical seismic reflection data from private entities. Given the shallow depth of the region, high-resolution gravity and magnetic data will also be essential for a thorough analysis. This may require precision measurements through ground surveys to accurately collect gravity and magnetic data. The study area is characterized by complex tectonic structures shaped by a diverse tectonic history. While the current study has focused on the Rangpur Saddle, future research will expand to cover the entire northwestern part of Bangladesh,



513 including the Himalayan Foredeep and the Eocene Hinge region, which represents a
514 Paleocoastal shelf. Such expanded coverage will provide deeper insights into the tectonic
515 evolution and geological complexity of the area.

516

517 **Conclusion**

518

519 This study provides a comprehensive geophysical investigation of the northwestern region of
520 Bangladesh, revealing its significant potential for mineral resource exploration. The integration of
521 gravity, magnetic, seismic, and drilling data has allowed us to identify key tectonic features, such
522 as gabbroic intrusions along extensional faults, which suggest the presence of valuable magnetic
523 mineral deposits. Despite the limitations in data resolution and coverage, our findings offer
524 important insights into the region's geological evolution and resource potential. Future work
525 should prioritize acquiring more detailed geophysical data and expanding drilling campaigns to
526 refine the understanding of subsurface structures and evaluate the feasibility of mineral extraction.
527 The Rangpur Saddle, as the shallowest part of the stable platform, emerges as a promising target
528 for future mineral exploration endeavors.

529

530 **Data availability**

531

532 All raw data can be provided by the corresponding authors upon request.

533

534 **Author contribution**

535

536 Mohammad Tawhidur Rahman Tushar was involved in conceptualization, methodology, software,
537 validation, formal analysis, investigation, resources, data curation, writing – original draft, writing
538 – review and editing, visualization. Asif Ashraf contributed to conceptualization, methodology,
539 software, validation, formal analysis, investigation, resources, data curation, writing – original
540 draft, writing – review and editing, and visualization. Md. Mahfuz Alam worked on software
541 development, validation, and formal analysis. Md Nasif Jamil contributed to writing – review and
542 editing and visualization. Saba Karim was involved in writing – review and editing and
543 visualization. Md. Shahjahan contributed to conceptualization, investigation, resources, project
544 administration, and supervision. Md. Anwar Hossain Bhuiyan was involved in writing – review
545 and editing, project administration, supervision, and funding acquisition.

546

547 **Competing interests**

548

549 The authors declare that they have no conflict of interest.

550

551 **Acknowledgment**

552

553 The gravity, magnetic, and seismic data, along with drilling information used in this study, were
554 graciously provided by the Geological Survey of Bangladesh (GSB), and the authors deeply
555 appreciate their support and collaboration. The authors also thank Asef Jamil Ajwad for his
556 assistance with computational facilities during the research. Special acknowledgment is made for
557 the Oasis Montaj classroom subscription and for the use of Geosoft Oasis Montaj v8.4 for data



558 processing and modeling. Finally, gratitude is extended to the Department of Geology, University
559 of Dhaka, for providing access to essential infrastructure and resources.

560

561 **Financial support**

562

563 This work was funded by the National Science and Technology Fellowship, awarded by the
564 Ministry of Science and Technology, Bangladesh.

565

566 **References**

567

568 Adebisi, L. S., Eluwole, A. B., Fajana, A. O., Salawu, N. B., and Saleh, A.: Contrasting structures
569 of the Southern Benue trough and the contiguous crystalline basement as observed from high-
570 resolution aeromagnetic data, *Sci Rep*, 13, 21516, <https://doi.org/10.1038/s41598-023-48639-8>,
571 2023.

572 Ahamed, S., Hossain, D., and Alam, J.: Exploring Basement Surface relationship of north-west
573 Bengal Basin using satellite images and tectonic modeling,
574 <https://doi.org/10.48550/ARXIV.2004.02734>, 2020.

575 Akhtar, A.: Mineral resources and their economic significance in national development:
576 Bangladesh perspective, *SP*, 250, 127–134, <https://doi.org/10.1144/GSL.SP.2005.250.01.12>,
577 2005.

578 Alam, M.: Geology and depositional history of Cenozoic sediments of the Bengal Basin of
579 Bangladesh, *Palaeogeography, Palaeoclimatology, Palaeoecology*, 69, 125–139,
580 [https://doi.org/10.1016/0031-0182\(89\)90159-4](https://doi.org/10.1016/0031-0182(89)90159-4), 1989.

581 Alam, M., Alam, M. M., Curray, J. R., Chowdhury, M. L. R., and Gani, M. R.: An overview of
582 the sedimentary geology of the Bengal Basin in relation to the regional tectonic framework and
583 basin-fill history, *Sedimentary Geology*, 155, 179–208, [https://doi.org/10.1016/S0037-0738\(02\)00180-X](https://doi.org/10.1016/S0037-0738(02)00180-X), 2003.

585 Alken, P., Thébaud, E., Beggan, C. D., Amit, H., Aubert, J., Baerenzung, J., Bondar, T. N., Brown,
586 W. J., Califf, S., Chambodut, A., Chulliat, A., Cox, G. A., Finlay, C. C., Fournier, A., Gillet, N.,
587 Grayver, A., Hammer, M. D., Holschneider, M., Huder, L., Hulot, G., Jager, T., Kloss, C., Korte,
588 M., Kuang, W., Kuvshinov, A., Langlais, B., Léger, J.-M., Lesur, V., Livermore, P. W., Lowes, F.
589 J., Macmillan, S., Magnes, W., Manda, M., Marsal, S., Matzka, J., Metman, M. C., Minami, T.,
590 Morschhauser, A., Mound, J. E., Nair, M., Nakano, S., Olsen, N., Pavón-Carrasco, F. J., Petrov,
591 V. G., Ropp, G., Rother, M., Sabaka, T. J., Sanchez, S., Saturnino, D., Schnepf, N. R., Shen, X.,
592 Stolle, C., Tangborn, A., Toffner-Clausen, L., Toh, H., Torta, J. M., Varner, J., Vervelidou, F.,
593 Vigneron, P., Wardinski, I., Wicht, J., Woods, A., Yang, Y., Zeren, Z., and Zhou, B.: International
594 Geomagnetic Reference Field: the thirteenth generation, *Earth Planets Space*, 73, 49,
595 <https://doi.org/10.1186/s40623-020-01288-x>, 2021.

596 Ameen, S. M. M., Wilde, S. A., Kabir, Md. Z., Akon, E., Chowdhury, K. R., and Khan, Md. S. H.:
597 Paleoproterozoic granitoids in the basement of Bangladesh: A piece of the Indian shield or an



- 598 exotic fragment of the Gondwana jigsaw?, *Gondwana Research*, 12, 380–387,
599 <https://doi.org/10.1016/j.gr.2007.02.001>, 2007.
- 600 Ameen, S. M. M., Tapu, A.-T., and Hossain, M. S.: Precambrian Basement Rock of Bangladesh
601 and Its Metallic Minerals, in: *Bangladesh geosciences and resources potential*, CRC Press Books,
602 25–54, 2021.
- 603 Anon: Geosoft, 2021.
- 604 Arkani-Hamed, J.: Differential reduction to the pole: Revisited, *GEOPHYSICS*, 72, L13–L20,
605 <https://doi.org/10.1190/1.2399370>, 2007.
- 606 Ashraf, A. and Filina, I.: New 2.75-D gravity modeling reveals the low-density nature of
607 propagator wakes in the Juan de Fuca plate, *Tectonophysics*, 869, 230127,
608 <https://doi.org/10.1016/j.tecto.2023.230127>, 2023a.
- 609 Ashraf, A. and Filina, I.: Zones of Weakness Within the Juan de Fuca Plate Mapped From the
610 Integration of Multiple Geophysical Data and Their Relation to Observed Seismicity, *Geochem*
611 *Geophys Geosyst*, 24, e2023GC010943, <https://doi.org/10.1029/2023GC010943>, 2023b.
- 612 Balogun, O. B., Akereke, O. F., and Nwobodo, A. D.: Understanding the Constraints to the Correct
613 Application of the Upward Continuation Operation in Gravity Data Processing, *Pure Appl.*
614 *Geophys.*, 180, 3787–3811, <https://doi.org/10.1007/s00024-023-03348-1>, 2023.
- 615 Brune, S., Kolawole, F., Olive, J.-A., Stamps, D. S., Buck, W. R., Buiter, S. J. H., Furman, T., and
616 Shillington, D. J.: Geodynamics of continental rift initiation and evolution, *Nat Rev Earth Environ*,
617 4, 235–253, <https://doi.org/10.1038/s43017-023-00391-3>, 2023.
- 618 Calvin, P., Ruiz-Martínez, V. C., Villalain, J. J., Casas-Sainz, A. M., and Moussaid, B.:
619 Emplacement and Deformation of Mesozoic Gabbros of the High Atlas (Morocco):
620 Paleomagnetism and Magnetic Fabrics, *Tectonics*, 36, 3012–3037,
621 <https://doi.org/10.1002/2017TC004578>, 2017.
- 622 Chowdhury, K. R., Hossain, M. S., and Khan, M. S. H. (Eds.): *Bangladesh geosciences and*
623 *resources potential*, First edition., CRC Press, Boca Raton, 610 pp., 2022.
- 624 Curray, J. R.: Geological history of the Bengal geosyncline, *Journal of Association of Exploration*
625 *Geophysicists*, 12, 209–219, 1991.
- 626 Curray, J. R. and Moore, D. G.: Sedimentary and Tectonic Processes in the Bengal Deep-Sea Fan
627 and Geosyncline, in: *The Geology of Continental Margins*, edited by: Burk, C. A. and Drake, C.
628 L., Springer Berlin Heidelberg, Berlin, Heidelberg, 617–627, [https://doi.org/10.1007/978-3-662-](https://doi.org/10.1007/978-3-662-01141-6_45)
629 [01141-6_45](https://doi.org/10.1007/978-3-662-01141-6_45), 1974.
- 630 DeCelles, P. G.: Foreland Basin Systems Revisited: Variations in Response to Tectonic Settings,
631 in: *Tectonics of Sedimentary Basins*, edited by: Busby, C. and Azor, A., Wiley, 405–426,
632 <https://doi.org/10.1002/9781444347166.ch20>, 2011.



- 633 Filina, I., Biegert, E. K., Sander, L., Tschirhart, V., Bundalo, N., and Schiek-Stewart, C.: Integrated
634 imaging: A powerful but undervalued tool, *The Leading Edge*, 38, 720–724,
635 <https://doi.org/10.1190/tle38090720.1>, 2019.
- 636 Fuller, R. E. and Waters, A. C.: The Nature and Origin of the Horst and Graben Structure of
637 Southern Oregon, *The Journal of Geology*, 37, 204–238, 1929.
- 638 Hasan, M. M., Monir, A., and Hassan, M.: Evaluating the Energy and Mineral Resources Prospect
639 and Future Development in Bangladesh: A Review, <https://doi.org/10.2139/ssrn.4484598>, 2023.
- 640 Hendrickson, M. D.: Geologic interpretation of aeromagnetic and chemical data from the Oaks
641 Belt, Wabigoon subprovince, Minnesota: implications for Au-rich VMS deposit exploration, *Can.
642 J. Earth Sci.*, 53, 176–188, <https://doi.org/10.1139/cjes-2015-0141>, 2016.
- 643 Hildenbrand, T. G.: Regional Crustal Structures and Their Relationship to the Distribution of Ore
644 Deposits in the Western United States, Based on Magnetic and Gravity Data, *Economic Geology*,
645 95, 1583–1603, <https://doi.org/10.2113/95.8.1583>, 2000.
- 646 Hossain, I., Tsunogae, T., Rajesh, H. M., Chen, B., and Arakawa, Y.: Palaeoproterozoic U–Pb
647 SHRIMP zircon age from basement rocks in Bangladesh: A possible remnant of the Columbia
648 supercontinent, *Comptes Rendus Geoscience*, 339, 979–986,
649 <https://doi.org/10.1016/j.crte.2007.09.014>, 2007.
- 650 Hossain, Md. S., Khan, Md. S. H., Chowdhury, K. R., and Abdullah, R.: Synthesis of the Tectonic
651 and Structural Elements of the Bengal Basin and Its Surroundings, in: *Tectonics and Structural
652 Geology: Indian Context*, edited by: Mukherjee, S., Springer International Publishing, Cham, 135–
653 218, https://doi.org/10.1007/978-3-319-99341-6_6, 2019.
- 654 Ibraheem, I. M., Tezkan, B., Ghazala, H., and Othman, A. A.: A New Edge Enhancement Filter
655 for the Interpretation of Magnetic Field Data, *Pure Appl. Geophys.*, 180, 2223–2240,
656 <https://doi.org/10.1007/s00024-023-03249-3>, 2023.
- 657 Jaffal, M., Goumi, N. E., Kchikach, A., Aïfa, T., Khattach, D., and Manar, A.: Gravity and
658 magnetic investigations in the Haouz basin, Morocco. Interpretation and mining implications,
659 *Journal of African Earth Sciences*, 58, 331–340, <https://doi.org/10.1016/j.jafrearsci.2010.03.012>,
660 2010.
- 661 Jain, A. K., Banerjee, D. M., and Kale, V. S.: *Tectonics of the Indian Subcontinent*, Springer
662 International Publishing, Cham, <https://doi.org/10.1007/978-3-030-42845-7>, 2020.
- 663 Kabir, Z. M., Chowdhury, K. R., Akon, E., Kazi, A. I., and Ameen, S. M. M.: Petrogenetic Study
664 of Precambrian Basement Rocks from Maddhapara, Dinajpur, Bangladesh, *Bangladesh
665 Geoscience Journal*, 7, 1–18, 2001.
- 666 Khan, A. A. and Rahman, T.: An analysis of the gravity field and tectonic evaluation of the
667 northwestern part of Bangladesh, *Tectonophysics*, 206, 351–364, [https://doi.org/10.1016/0040-
668 1951\(92\)90386-K](https://doi.org/10.1016/0040-1951(92)90386-K), 1992.



- 669 Khan, F. H.: Geology of Bangladesh, 1991.
- 670 Kharbish, S., Eldosouky, A. M., and Amer, O.: Integrating mineralogy, geochemistry and
671 aeromagnetic data for detecting Fe–Ti ore deposits bearing layered mafic intrusion, Akab El-
672 Negum, Eastern Desert, Egypt, *Sci Rep*, 12, 15474, <https://doi.org/10.1038/s41598-022-19760-x>,
673 2022.
- 674 Kheyrollahi, H., Alinia, F., and Ghods, A.: Regional magnetic and gravity structures and
675 distribution of mineral deposits in Central Iran: Implications for mineral exploration, *Journal of*
676 *Asian Earth Sciences*, 217, 104828, <https://doi.org/10.1016/j.jseas.2021.104828>, 2021.
- 677 Ma, G., Huang, D., and Liu, C.: Step-Edge Detection Filters for the Interpretation of Potential
678 Field Data, *Pure Appl. Geophys.*, 173, 795–803, <https://doi.org/10.1007/s00024-015-1053-6>,
679 2016.
- 680 Magee, C., Ernst, R. E., Muirhead, J., Phillips, T., and Jackson, C. A.: Magma transport pathways
681 in large igneous provinces: lessons from combining field observations and seismic reflection data,
682 in: *Dyke Swarms of the World: A Modern Perspective*, 45–85, 2019.
- 683 Masum, M., Hoque, M. N., Akbar, M. A., Mahmud, Z., Rana, M. S., Razzaque, M. A., and Amin,
684 M. A.: Geology and Precambrian Banded Iron Formation formed at Rangpur Platform in
685 Bangladesh, *International Journal Of Engineering Research And Development*, 17, 43–57, 2021.
- 686 McCafferty, A. E., Stoesser, D. B., and Van Gosen, B. S.: Geophysical interpretation of U, Th, and
687 rare earth element mineralization of the Bokan Mountain peralkaline granite complex, Prince of
688 Wales Island, southeast Alaska, *Interpretation*, 2, SJ47–SJ63, <https://doi.org/10.1190/INT-2014-0010.1>, 2014.
- 690 Mohamed, A., Abdelrady, M., Alshehri, F., Mohammed, M. A., and Abdelrady, A.: Detection of
691 Mineralization Zones Using Aeromagnetic Data, *Applied Sciences*, 12, 9078,
692 <https://doi.org/10.3390/app12189078>, 2022.
- 693 Moon, J. W.: *The Mineral Industry of Bangladesh*, U.S. Geological Survey, 2022.
- 694 Morgan, J. P. and McINTIRE, W. G.: QUATERNARY GEOLOGY OF THE BENGAL BASIN,
695 EAST PAKISTAN AND INDIA, *Geol Soc America Bull*, 70, 319, [https://doi.org/10.1130/0016-7606\(1959\)70\[319:QGOTBB\]2.0.CO;2](https://doi.org/10.1130/0016-7606(1959)70[319:QGOTBB]2.0.CO;2), 1959.
- 697 Mousa, S. A. W., Abdel Nabi, S. H., Araffa, S. A. S., Mansour, S. A., and Al Deep, M. A. I.:
698 Geophysical exploration of titanomagnetite ore deposits by geomagnetic and geoelectric methods,
699 *SN Appl. Sci.*, 2, 444, <https://doi.org/10.1007/s42452-020-2206-5>, 2020.
- 700 Nabighian, M. N.: THE ANALYTIC SIGNAL OF TWO-DIMENSIONAL MAGNETIC BODIES
701 WITH POLYGONAL CROSS-SECTION: ITS PROPERTIES AND USE FOR AUTOMATED
702 ANOMALY INTERPRETATION, *GEOPHYSICS*, 37, 507–517,
703 <https://doi.org/10.1190/1.1440276>, 1972.



- 704 Nasuti, Y., Nasuti, A., and Moghadas, D.: STDR: A Novel Approach for Enhancing and Edge
705 Detection of Potential Field Data, *Pure Appl. Geophys.*, 176, 827–841,
706 <https://doi.org/10.1007/s00024-018-2016-5>, 2019.
- 707 Núñez-Demarco, P., Bonilla, A., Sánchez-Bettucci, L., and Prezzi, C.: Potential-Field Filters for
708 Gravity and Magnetic Interpretation: A Review, *Surv Geophys*, 44, 603–664,
709 <https://doi.org/10.1007/s10712-022-09752-x>, 2023.
- 710 Ogah, A. J. and Abubakar, F.: Solid mineral potential evaluation using integrated aeromagnetic
711 and aeroradiometric datasets, *Sci Rep*, 14, 1637, <https://doi.org/10.1038/s41598-024-52270-6>,
712 2024.
- 713 Pham, L. T. and Oliveira, S. P.: Edge Enhancement of Magnetic Sources Using the Tilt Angle and
714 Derivatives of Directional Analytic Signals, *Pure Appl. Geophys.*, 180, 4175–4189,
715 <https://doi.org/10.1007/s00024-023-03375-y>, 2023.
- 716 Pirajno, F. and Santosh, M.: Rifting, intraplate magmatism, mineral systems and mantle dynamics
717 in central-east Eurasia: An overview, *Ore Geology Reviews*, 63, 265–295,
718 <https://doi.org/10.1016/j.oregeorev.2014.05.014>, 2014.
- 719 Rahman, Md. M. and Ullah, S. E.: Inversion of Gravity Data for Imaging of a Sediment-basement
720 Interface: A Case Study in the Northwestern Part of Bangladesh, *Pure Appl. Geophys.*, 166, 2007–
721 2019, <https://doi.org/10.1007/s00024-009-0530-1>, 2009.
- 722 Reimann, K. U. and Hiller, K.: *Geology of Bangladesh*, 1993.
- 723 Roest, W. R. and Pilkington, M.: Identifying remanent magnetization effects in magnetic data,
724 *GEOPHYSICS*, 58, 653–659, <https://doi.org/10.1190/1.1443449>, 1993.
- 725 Roy, A. B. and Chatterjee, A.: Tectonic framework and evolutionary history of the Bengal Basin
726 in the Indian subcontinent, *Current Science*, 109, 271–279, 2015.
- 727 Royhan Gani, M. and Mustafa Alam, M.: Sedimentation and basin-fill history of the Neogene
728 clastic succession exposed in the southeastern fold belt of the Bengal Basin, Bangladesh: a high-
729 resolution sequence stratigraphic approach, *Sedimentary Geology*, 155, 227–270,
730 [https://doi.org/10.1016/S0037-0738\(02\)00182-3](https://doi.org/10.1016/S0037-0738(02)00182-3), 2003.
- 731 Ruppel, C.: Extensional processes in continental lithosphere, *J. Geophys. Res.*, 100, 24187–24215,
732 <https://doi.org/10.1029/95JB02955>, 1995.
- 733 Smith, W. H. F. and Sandwell, D. T.: Global Sea Floor Topography from Satellite Altimetry and
734 Ship Depth Soundings, *Science*, 277, 1956–1962, <https://doi.org/10.1126/science.277.5334.1956>,
735 1997.
- 736 Sundararajan, N.: A General Perspective on Geophysical Methods in Mineral Exploration, in: *On*
737 *a Sustainable Future of the Earth’s Natural Resources*, 53–83, 2012.



- 738 Thompson, J. O., Moulin, M., Aslanian, D., De Clarens, P., and Guillocheau, F.: New starting
739 point for the Indian Ocean: Second phase of breakup for Gondwana, *Earth-Science Reviews*, 191,
740 26–56, <https://doi.org/10.1016/j.earscirev.2019.01.018>, 2019.
- 741 Troll, V. R., Mattsson, T., Upton, B. G. J., Emeleus, C. H., Donaldson, C. H., Meyer, R., Weis, F.,
742 Dahrén, B., and Heimdal, T. H.: Fault-Controlled Magma Ascent Recorded in the Central Series
743 of the Rum Layered Intrusion, NW Scotland, *Journal of Petrology*, 61, egaa093,
744 <https://doi.org/10.1093/petrology/egaa093>, 2021.
- 745 Uddin, A. and Lundberg, N.: Unroofing history of the eastern Himalaya and the Indo-Burman
746 ranges; heavy-mineral study of Cenozoic sediments from the Bengal Basin, Bangladesh, *Journal*
747 *of Sedimentary Research*, 68, 465–472, <https://doi.org/10.2110/jsr.68.465>, 1998.
- 748 Valdiya, K. S.: *The Making of India*, Springer International Publishing, Cham,
749 <https://doi.org/10.1007/978-3-319-25029-8>, 2016.
- 750 Veevers, J. J.: Gondwanaland from 650–500 Ma assembly through 320 Ma merger in Pangea to
751 185–100 Ma breakup: supercontinental tectonics via stratigraphy and radiometric dating, *Earth-*
752 *Science Reviews*, 68, 1–132, <https://doi.org/10.1016/j.earscirev.2004.05.002>, 2004.
- 753 Zhang, H., Greco, F., Sacek, V., Geng, M., and Liu, P.: Editorial: Applications of gravity
754 anomalies in geophysics, *Front. Earth Sci.*, 12, 1349161,
755 <https://doi.org/10.3389/feart.2024.1349161>, 2024.
- 756 Zhang, S., Li, Z.-X., Evans, D. A. D., Wu, H., Li, H., and Dong, J.: Pre-Rodinia supercontinent
757 Nuna shaping up: A global synthesis with new paleomagnetic results from North China, *Earth and*
758 *Planetary Science Letters*, 353–354, 145–155, <https://doi.org/10.1016/j.epsl.2012.07.034>, 2012.
- 759 Zhou, M.-F., Robinson, P. T., Leshner, C. M., Keays, R. R., Zhang, C.-J., and Malpas, J.:
760 Geochemistry, Petrogenesis and Metallogenesis of the Panzhihua Gabbroic Layered Intrusion and
761 Associated Fe–Ti–V Oxide Deposits, Sichuan Province, SW China, *Journal of Petrology*, 46,
762 2253–2280, <https://doi.org/10.1093/petrology/egi054>, 2005.

763